Atmos. Chem. Phys. Discuss., 15, 16715–16745, 2015
www.atmos-chem-phys-discuss.net/15/16715/2015/
doi:10.5194/acpd-15-16715-2015

Atmospheric Chemistry and Physics
Discussions
Open Access

Sea salt aerosols as a reactive surface for inorganic and organic acidic gases in the arctic troposphere

J. W. Chi[1], W. J. Li[1], D. Z. Zhang[2], J. C. Zhang[3], Y. T. Lin[3], X. J. Shen[4], J. Y. Sun[4], J. M. Chen[1], X. Y. Zhang[4], Y. M. Zhang[4], and W. X. Wang[1]

[1]Environment Research Institute, Shandong University, Jinan, Shandong 250100, China
[2]Faculty of Environmental and Symbiotic Sciences, Prefectural University of Kumamoto, Kumamoto 862-8502, Japan
[3]Key Laboratory of the Earth' Deep Interior, Institute of Geology and Geophysics, Chinese Academy of Sciences, Beijing 100029, China
[4]Key Laboratory of Atmospheric Chemistry of CMA, Institute of Atmospheric Composition, Chinese Academy of Meteorological Sciences, Beijing 100081, China

Received: 24 May 2015 – Accepted: 26 May 2015 – Published: 18 June 2015

Correspondence to: J. W. Chi (liweijun@sdu.edu.cn)
and Y. M. Zhang (ymzhang@cams.cma.gov.cn)

Published by Copernicus Publications on behalf of the European Geosciences Union.

Abstract

Sea salt aerosols (SSA) are dominant particles in the arctic atmosphere and determine the polar radiative balance. SSA react with acidic pollutants that lead to changes of physical and chemical properties of their surface, which in turn alter their hygroscopic and optical properties. Transmission electron microscopy with energy-dispersive X-ray spectrometry was used to analyze morphology, composition, size, and mixing state of individual SSA at Ny-Ålesund, Svalbard in summertime. Individual fresh SSA contained cubic NaCl coated by certain amounts of $MgCl_2$ and $CaSO_4$. Individual partially aged SSA contained irregular NaCl coated by a mixture of $NaNO_3$, Na_2SO_4, $Mg(NO_3)_2$, and $MgSO_4$. The comparison suggests the hydrophilic $MgCl_2$ coating in fresh SSA likely intrigued the heterogeneous reactions at the beginning of SSA and acidic gases. Individual fully aged SSA normally had Na_2SO_4 cores and an amorphous coating of $NaNO_3$. Elemental mappings of individual SSA particles revealed that as the particles ageing Cl gradually decreased but the C, N, O, and S content increased. $^{12}C^{14}N^-$ mapping from nanoscale secondary ion mass spectrometry indicates that organic matter increased in the aged SSA compared with the fresh SSA. $^{12}C^{14}N^-$ line scans further show that organic matter was mainly concentrated on the aged SSA surface. These new findings indicate that this mixture of organic matter and $NaNO_3$ on particle surfaces determines their hygroscopic and optical properties. These abundant SSA, whose reactive surfaces absorb inorganic and organic acidic gases in the arctic troposphere, need to be incorporated into atmospheric chemical models.

1 Introduction

The arctic atmosphere was long believed to be an extremely clean background laboratory to research aerosol chemical processes, transport of atmospheric aerosols, and their impact on global climate (Law and Stohl, 2007). In the last decades, however, arctic temperatures have increased at twice the global average rate (Serreze and Francis, 2006), resulting in a dramatic decrease of Arctic pack ice (Lindsay et al., 2009). This arctic climate change has been attributed to the increase of greenhouse gases in the troposphere (Vavrus, 2004) and to anthropogenic emissions of air pollutants from the middle latitudes (Barrie, 1986; Iziomon et al., 2006; Law and Stohl, 2007). In particular, the "Arctic Haze" phenomenon caused by the long-range transport of anthropogenic emissions (e.g., organic acids, H_2SO_4/SO_2, and HNO_3/NO_2) from lower latitudes has received increasing attention in the last thirty years (Heintzenberg, 1980; Shaw, 1995; Law and Stohl, 2007).

Various aerosol particles from industrial, urban, and marine emissions occur in the arctic atmosphere (Goto-Azuma and Koerner, 2001; Ghorai et al., 2014). Black carbon as one solar absorber in the troposphere and in the snow or ice (Hegg et al., 2009) can amplify the change of the arctic climate (Sand et al., 2013). In addition, H_2SO_4/SO_2 and HNO_3/NO_2 from anthropogenic sources in middle latitudes are transported into the central arctic area (Law and Stohl, 2007), where they react with sea salt aerosols (SSA) (Hara et al., 2003; Geng et al., 2010; Sierau et al., 2014). SSA have reactive surfaces that can easily participate in heterogeneous and multiphase chemical reactions (Rossi, 2003) and play a significant role in the global S and N cycle (Pósfai et al., 1994; Sierau et al., 2014). These aged SSA not only affect incoming solar radiation by scattering or absorbing directly (Murphy et al., 1998), but also can serve as cloud condensation nuclei (CCN) or ice nuclei (IN) and further alter cloud properties (Hu et al., 2005; Leck and Svensson, 2015). It was also proved that such cloud changes cause 40 % of the arctic warming (Vavrus, 2004). Understanding the chemical composition of the arctic SSA is critical to understand how they affect the polar climate (Hara et al., 2003).

SSA have been intensively studied in both laboratory and field experiments in coastal areas (O'Dowd et al., 1997; O'Dowd and De Leeuw, 2007; Yao and Zhang, 2011; Li et al., 2011b; Laskin et al., 2012; Ault et al., 2012; Ghorai et al., 2014). In laboratory studies Ault et al. (2013a) suggested spatial redistribution of the cations (Na^+, K^+, Mg^{2+}, and Ca^{2+}) between core and surface after heterogeneous reaction of SSA and nitric acids. Deliquescence-mode experiments with mixed NaCl/$MgSO_4$ aerosol particles show that Mg salts (e.g., $MgSO_4$ and $MgCl_2$) concentrated in the surface can easily take up water and lower the deliquescence point of NaCl particles (Woods et al., 2010). Hara et al. (2003) suggested that most SSA play a pivotal pole in the lower troposphere (< 3 km) and result in noticeable depletion of chlorine in the arctic. Recently, Laskin et al. (2012) found that SSA may effectively react with organic acids, leaving behind particles depleted in chloride and enriched in the corresponding organic salts in one polluted coastal area. Organic acids can react with SSA and change their hygroscopicity in polluted continental air (Ghorai et al., 2014), which can alter their heterogeneous reactions and CCN activity (Laskin et al., 2012). In light of the limited microscopic observations of arctic aerosols, at least two questions have not been answered. Firstly, detailed information about ageing processes of SSA surfaces has not been determined in the arctic atmosphere. Secondly, to what degree do organic acids react with SSA in the arctic atmosphere? This knowledge is critical to understand how small amounts of anthropogenic gases (e.g., organic acids, H_2SO_4/SO_2, and HNO_3/NO_2) affect the hygroscopic and optical properties of SSA in the clean arctic atmosphere.

To characterize individual SSA collected on 3–23 August 2012, at the Chinese Arctic Yellow River Station, we applied different microscopic techniques with resolution down to the nanometer scale: transmission electron microscopy with energy-dispersive X-ray spectrometry (TEM/EDX), scanning electron microscopy (SEM), scanning TEM (STEM), and atomic force microscopy (AFM), and nanoscale secondary ion mass spectrometry (nanoSIMS). The different types of individual SSA were identified based on their morphology and composition. Elemental and ion mappings revealed mixing properties of different species in individual SSA which further participated in chemical reactions in the clean Arctic atmosphere. The dual aims of our study are to explain the need to understand the complexity of realistic atmospheric SSA and to provide fundamental experimental data to understand heterogeneous reactions of SSA in the clean arctic atmosphere.

2 Experiments

2.1 Sampling

Svalbard is an archipelago in the Arctic Ocean consisting of Spitsbergen, Bear Island, and Hopen, which together cover about 62 000 km^2. Ny-Ålesund, whose geographical coordinates are 78°55′ N, 11°56′ E, is situated on the west coast of Spitsbergen and is an international center of scientific research and environmental monitoring in the central Arctic.

Aerosol samples were collected from 3 to 23 August 2012, using an individual particle sampler at the Chinese Arctic Yellow River Station, Ny-Ålesund (Fig. S1). We use copper TEM grids coated with carbon film (carbon type-B, 300-mesh copper, Tianld Co., China) to collect aerosols by a single-stage cascade impactor with a 0.5-mm-diameter jet nozzle at a flow rate of 1.0 L min^{-1}. The sampling duration of each sample varied from twenty minutes to two hours depending on the aerosol dispersion on the film that was estimated by optical microscopy after the sampling. Then we placed the grids in sealed, dry, plastic capsules to prevent contamination. Finally, the samples were stored in a desiccator at 25 °C and 20 ± 3 % RH until analysis (Li et al., 2011a).

According to the sampling time and sample quality, 23 aerosol samples were selected for analysis with TEM. During the sampling periods, temperatures were 1.6–7.3 °C; relative humidity, 56–94 %; air pressure, 997.0–1020.7 hPa; and sampling wind speeds, 0–8.9 m s^{-1}. Detailed sampling information can be found in Table S1. Three-day (72 h) backward air mass trajectories were generated with the HYSPLIT model from the Chinese Arctic Yellow River Station during 3–23 August 2012, at an altitude of 500 m above the sea level (Fig. 1). Most of the air masses originated in the Arctic Ocean, including four from Canada or Greenland, and were restricted to this vast marine region during the sampling periods.

2.2 Electron microscopic analyses

Individual particle samples were examined by a JEOL JEM-2100 transmission electron microscopy operated at 200 kV with energy-dispersive X-ray spectrometry (TEM/EDX) and scanning electron microscopy (SEM; Philips XL30) operated at a 20 kV accelerating voltage and a 80 µA filament. EDX spectra were examined within a maximum time of 30 s to minimize potential beam damage and efficiently collect particle elemental composition. TEM grids were made of copper (Cu) and covered by a carbon-reinforced substrate, so Cu had to be excluded from the quantitative analyses of the particles while residual C content was detected and overestimated in EDX spectra of individual particles. Elemental composition, morphology, size distribution, and mixing state have been studied by the TEM/EDX. Both submicron and supermicron particles occur on the TEM grids: coarser particles occur near the center, and finer particles are on the periphery (Li and Shao, 2009). To be more representative, 4–5 areas from the center to periphery of the sampling spot were chosen to analyze all the particles. Altogether we analyzed 1577 aerosol particles to understand the details of their mixing states, both internal and external. We used iTEM software to analyze the TEM images and obtained area, circularity, perimeter, and equivalent circle diameter of individual aerosol particles.

Some typical aerosol particles were analyzed for elemental mapping with a JEOL JEM-2100F TEM with scanning TEM (STEM) operation mode. Elemental mappings were collected in the annular dark-field imaging mode, with the electron beam focused on a corresponding spot of the sample but then scanned over this area in a raster. Elemental mapping has become an important tool in single-particle analysis in the recent years (Ault et al., 2012; Li et al., 2013a, b), because it clearly displays the distribution of the detectable elements within each particle.

2.3 NanoSIMS analysis

Individual aerosol particles were analyzed using a nanoscale secondary ion mass spectrometer (nanoSIMS) 50 L (CAMECA Instruments, Geneviers, France), an ultra-high vacuum technique for surface and thin-film analysis at the Institute of Geology and Geophysics, Chinese Academy of Sciences. In this study, $^{16}O^-$, $^{12}C^{14}N^-$, $^{32}S^-$, $^{35}Cl^-$, and $^{16}O^{23}Na^-$ ions in individual particles were obtained when the Cs^+ primary ion beam caused the ionization of atoms within the particles. Furthermore, ion intensity mappings of individual particles with nanometer resolution can show the distribution of different ions. $^{12}C^{14}N^-$ represents the organic matter in individual particles that excludes the contribution from the carbon substrate.

2.4 AFM analysis

Atomic force microscopy (AFM) with a tapping mode analyzed aerosol particles under ambient conditions. AFM, a digital NanoscopeIIIa Instrument, can detect the three-dimensional morphology of particles. The AFM settings contain imaging forces between 1 and 1.5 nN, scanning rates between 0.5 and 0.8 Hz, and scanning range sizes at 10 µm with a resolution of 512 pixels per length. After the AFM analysis, composition of the same particles was confirmed by TEM, with nineteen SSA particles analyzed by this method. The NanoScope analysis software can automatically obtain bearing area (A) and bearing volume (V) of each analyzed particle according to the following formula.

$$A = \frac{4}{3}\pi r^2 = \frac{\pi d^2}{4} \rightarrow d = \sqrt{\frac{4A}{\pi}} \tag{1}$$

$$V = \frac{4}{3}\pi r^3 = \frac{4}{3} \times \frac{\pi D^3}{8} \rightarrow D = \sqrt[3]{\frac{6V}{\pi}} \tag{2}$$

Where d is the equivalent circle diameter and D the equivalent spherical diameter.

Additionally, we know the relation between d and D is $D = 0.7487 \times d$, as shown in Fig. S2. As a result, equivalent circle diameter (d) of individual aerosol particles measured from the iTEM software can be further converted into equivalent spherical diameter (D) based on this relationship.

3 Results

3.1 Types and size distribution of Arctic aerosol particles

Based on their different morphology and composition, aerosol particles were divided into four major categories: sea salt (Fig. 2a-a), S-rich (OC-coating) (Fig. 2a–b), Ca / Mg-S / N / Cl (Fig. 2a-c) and mineral (Fig. 2a–d). TEM observations indicated that SSA were most abundant from 100 nm to 10 µm in the summer arctic atmosphere. Figure 2b shows that the relative abundance of SSA in the samples was about 72 % of the total aerosol. This result is consistent with 70–80 % SSA in different seasons reported for the arctic atmosphere (Hara et al., 2003; Geng et al., 2010).

3.2 The microscopic characterization and elements of SSA

Based on their morphology and composition, we can further identify three types of SSA: fresh SSA, partially aged SSA, and fully aged SSA.

3.2.1 Fresh SSA

The fresh SSA refer to particles which don't experience any atmospheric chemical modification after emission. TEM images clearly show that individual fresh SSA include the cubic NaCl core with $MgCl_2$ and $CaSO_4$ coating. Figure 3i shows that the NaCl core only contains Na and Cl with their ionic concentration ratio (Na/Cl) at 1 : 1. The coating contains appropriate quantities of Mg, Ca, S, O and Cl, which could be defined as $CaSO_4$, $MgCl_2$, and other species (Fig. 3j, k, l). NaCl particles surrounded by the Mg-rich and Ca-rich coatings have been inferred by SEM and TEM (Pósfai et al., 1994; Murphy et al., 1998; Hara et al., 2003; Geng et al., 2010), but the details about the coatings have not been revealed in the Arctic atmosphere. In this study, the high-resolution TEM images displayed the accurate mixing structures of NaCl and other species. Here we identified two kinds of fresh SSA: one, a NaCl core encased by a distinct coating of $CaSO_4$ and Mg-rich ($MgCl_2$) materials (e.g., Fig. 3a–d); and another, a NaCl core encased by a mixture of Mg-rich and Ca-rich materials (e.g., Fig. 3e–f).

3.2.2 Partially aged SSA

Partially aged SSA, we define as those particles that experience atmospheric chemical modifications on their surfaces but retain their NaCl core. Figure 4a-f shows that individual partially aged SSA clearly include NaCl core and coating. The morphology of the partially aged SSA differ from the fresh ones as shown in the TEM images of Figs. 3 and 4. Figure 4 shows that the core still keeps the crystalline phase of NaCl with its irregular shape and that the coatings mainly consist of Na, Mg, Ca, K, O, and S with either negligible or minor Cl. Typical Cl-depletion phenomena suggest that the SSA likely underwent chemical ageing in the atmosphere, as below:

$$MgCl_{2(\text{s or aq})} + HNO_{3(\text{g or aq})} \rightarrow Mg(NO_3)_{2(\text{aq})} + HCl_{(\text{g or aq})} \tag{R1}$$

$$MgCl_{2(\text{s or aq})} + H_2SO_{4(\text{g or aq})} \rightarrow MgSO_{4(\text{aq})} + HCl_{(\text{g or aq})} \tag{R2}$$

$$NaCl_{(\text{s or aq})} + HNO_{3(\text{g or aq})} \rightarrow NaNO_{3(\text{aq})} + HCl_{(\text{g or aq})} \tag{R3}$$

$$NaCl_{(\text{s or aq})} + H_2SO_{4(\text{g or aq})} \rightarrow Na_2SO_{4(\text{aq})} + HCl_{(\text{g or aq})} \tag{R4}$$

(s, solid; aq, aqueous; and g, gaseous)

Similar chemical reactions on SSA have been detected in both coastal air and laboratory experiments (Allen et al., 1996; Gard et al., 1998; Kouyoumdjian and Saliba, 2006; Ault et al., 2013a). These heterogeneous chemical reactions significantly change the morphology and composition of SSA. Our results suggest that the $MgCl_2$ coatings in fresh SSA were converted into a more complex coating mixture of $MgSO_4$, $Mg(NO_3)_2$, Na_2SO_4, and $NaNO_3$ in partially aged SSA.

3.2.3 Fully aged SSA

In fully aged SSA the NaCl core has been completely transformed into $NaNO_3$ and Na_2SO_4 through atmospheric heterogeneous chemical reactions with acidic gases. Figure 5 shows that the fully aged SSA have completely lost their NaCl core, suggesting that the Cl in SSA was completely depleted through heterogeneous chemical reactions, such as Reactions (R1)–(R4). The rod-like Na_2SO_4 aggregates comprising the core were frequently internally mixed with $NaNO_3$. TEM study indicates that Na_2SO_4 and $NaNO_3$ are crystalline and amorphous materials, respectively. Individual particles (Fig. 5) become more round compared with fresh SSA (Fig. 3) and partially aged SSA (Fig. 4), suggesting that the aged SSA tend to be droplets in ambient air.

3.3 Size distribution of individual SSA

Figure 6 shows size distributions of the fresh, partially aged, and fully aged SSA. The peaks of fresh and partially aged SSA are 0.68 and 1.30 µm, respectively, and the fully aged ones display a broad size range from 0.9 to 2.0 µm (Fig. 6). Our results show that the average particle sizes gradually increase as the SSA ageing. Therefore, the dry and wet depositions of aerosol particles could be changed following the degree of the particles ageing.

4 Discussion

4.1 Sulfate and nitrate formation in individual SSA

TEM observations classified the SSA into fresh, partially aged, and fully aged SSA in the arctic atmosphere. Using single particle analysis of the three types of SSA, it is shown that there is a major change of their internal structure and composition as the particles ageing. The STEM further determined elemental mappings of Na, Mg, Ca, Cl, S, O, C, and N in the three kinds of SSA. Elemental mapping can clearly display the elemental distribution within each particle, which indicates the possible heterogeneous chemical reactions on their surfaces (Conny and Norris, 2011; Ault et al., 2012). Figure 7 shows that Cl content decreases and S, O, C and N contents increase as the particles ageing: from partially aged (particle B) to fully aged SSA (particle C). This result provides direct evidence that sulfate and nitrate accumulated in SSA through atmospheric chemical reactions (e.g., Reactions R1–R4) in the arctic area. Moreover, this result is consistent with the TEM/EDX results shown in Figs. 3–5 and with investigators who found that individual SSA in the Arctic air contained certain amounts of sulfate or nitrate by SEM/EDX and aerosol time-of-flight mass spectrometry (ATOFMS) (Hara et al., 2003; Geng et al., 2010; Sierau et al., 2014). However, we found that individual aged particles simultaneously contained sulfate and nitrate, suggesting individual SSA underwent heterogeneous reactions with different acidic gases during ageing processes in the arctic atmosphere. A number of studies found that a large fraction of SSA internally mixed with sulfate and nitrate occurred from coastal to background marine air and from equatorial to high latitudes (Andreae et al., 1986; Pósfai et al., 1994; Middlebrook et al., 1998; Hara et al., 2003; Geng et al., 2010; Li et al., 2011b; Yao and Zhang, 2011; Laskin et al., 2012). Interestingly, we found that particle C had an elevated carbon content (Fig. 7), suggesting that organic matter might occur in the aged SSA. Recently, Laskin et al. (2012) showed that SSA can react with secondary organic acids and result in formation of organic salts in the atmosphere.

Na mappings show that Na is absent in the coating of particle A but is present in minor amounts in the coating of particle B (Fig. 7), which is consistent with the EDX results as shown in Figs. 3–4. In contrast, Mg, S, and O are absent from the core of particle A but are present in certain amounts within the core of particle B (Fig. 7). Therefore, we can deduce that $MgCl_2$ coatings of the fresh SSA firstly reacted with acidic gases through chemical Reactions (R1) and (R2) as the fresh SSA were transformed into the partially aged SSA. The presence of $MgCl_2$ coatings in the fresh SSA is particularly interesting because it is known to readily deliquesce at a point considerably lower (33 % RH at 298 K) than that of NaCl (75 %) (Wise et al., 2009). We conclude, therefore, that this $MgCl_2$ coating consistently allowed an aqueous layer to coat the fresh SSA in the Arctic atmosphere, because the ambient relative humidity (56–94 %) exceeded the deliquescence point. Despite the relatively low concentration of $MgCl_2$ in SSA, the liquid surface significantly enhances heterogeneous reactions rates through the uptake of acidic gases (e.g., H_2SO_4/SO_2, and HNO_3/NO_2) (Liu et al., 2007). Microscopic observations suggest that $MgCl_2$ on fresh SSA likely initiated and promoted the heterogeneous reactions between SSA and acidic gases. To our knowledge, this is the first demonstration of the influence of minor $MgCl_2$ in individual SSA in field studies, although this phenomenon has been reported in laboratory experiments (Zhao et al., 2006; Liu et al., 2007; Wise et al., 2009). In addition, $MgCl_2$ appears to have greater importance in individual Arctic SSA than elsewhere because the Mg^{2+}/Na^+ ratio in SSA increases following a temperature decrease (Hara et al., 2012). In the partially aged particles, the new coating containing $MgSO_4$, $Mg(NO_3)_2$, and $NaNO_3$ (Fig. 4) typically remained as a supersaturated liquid coating on the surface of the ambient SSA in the arctic area (Zhao et al., 2006; Li et al., 2008; Woods et al., 2010). Therefore, the Mg-salts in fresh and partially aged SSA are important surfactants to speed up particles ageing in the arctic area.

In this study we found an abundance of fully aged SSA in this arctic area (Figs. 5 and 6). Ault et al. (2013a) found that the Na^+, Mg^{2+} and Ca^{2+} in individual SSA undergo a spatial redistribution after heterogeneous reaction with nitric acid in the laboratory. We noticed a similar phenomenon in which Na, Mg, and Ca mappings in particle C were different from particles A and B (Fig. 7). Na is enhanced at the surface; Mg and Ca tend to concentrate in the individual particle center. Figure 7 shows that carbon intensity becomes strong in particle C, similar to the C-rich coating in Fig. 5c and d. These results suggest that the aged SSA probably contain organic matter (the details in Sect. 4.2). In addition, most of the fully aged SSA have a Na_2SO_4 core coated with

$NaNO_3$ (with minor $Mg(NO_3)_2$ and $MgSO_4$) (Fig. 5). As a result, the amorphous $NaNO_3$ coating totally determines particle hygroscopic and optical properties of the fully aged SSA. $NaNO_3$ can take up water starting at 25 % RH and grow continuously with increasing RH (Lee and Hsu, 2000). Hu et al. (2010) also illustrated that $NaNO_3$ did not exhibit obvious deliquescence phenomenon in the hygroscopic experiment. We conclude that the partially and fully aged Arctic SSA had liquid surfaces in ambient air (56–94 % RH) and that this liquid amounted to a substantial quantity of water in these aerosol particles. Park et al. (2014) supplied the evidence of water in the particles through the hygroscopicity and volatility tandem differential mobility analyzer. The hygroscopic growth of particles can cause 1.6 to 3.7 times more negative aerosol direct radiative effects (Sand et al., 2013) than particles without it.

Our results indicate that formation of sulfate and nitrate in the SSA can remove trace gases (e.g., H_2SO_4/SO_2, and HNO_3/NO_2) in the arctic air, which were mostly emitted by various anthropogenic sources from middle latitudes (Law and Stohl, 2007; Chang et al., 2011). On the one hand, the results of these heterogeneous reactions could change the CCN or IN abilities, optical properties, and further dry and wet deposition of SSA. On the other hand, the heterogeneous reactions on SSA surfaces can release gaseous $ClNO_2$ into arctic air, important for photochemical reactions in the Arctic (Oum et al., 1998; De Haan et al., 1999). These surface reactions of SSA could reduce the overall photochemical reactivity of the Arctic air because they release halogen species (Cl_2) (De Haan et al., 1999; Knipping et al., 2000).

4.2 Organic matter in aged SSA

TEM observations provided direct evidence of sulfate and nitrate formation in aged SSA through heterogeneous reactions with H_2SO_4/SO_2, and HNO_3/NO_2 in the arctic area. Recently, Laskin et al. (2012) showed that SSA effectively reacted with organic acids in polluted coastal air, leaving behind particles depleted in chloride and enriched in the corresponding organic salts. However, whether weak organic acids participated in the chloride depletion remains uncertain in the clean arctic air. NanoSIMS technology has been adopted to characterize secondary ion intensity mappings of $^{32}S^-$, $^{12}C^{14}N^-$, $^{23}Na^{16}O^-$, $^{35}Cl^-$, and $^{16}O^-$. In this study, $^{12}C^{14}N^-$ was selected to indicate organic matter in SSA (Fig. 8).

Figure 8a shows that $^{35}Cl^-$ in the NaCl core and minor $^{16}O^-$ and $^{32}S^-$ in the coating in particle 1 suggest that this SSA particle is fresh. Figure 8b shows in particles 2 and 3 that the absence of $^{35}Cl^-$ and the high intensity of $^{32}S^-$, $^{23}Na^{16}O^-$, and $^{16}O^-$, and these are fully aged particles. These results are completely consistent with the TEM observations above. $^{12}C^{14}N^-$ mapping and line scan of particle 1 together indicate extremely small amounts of organic matter in the coating of the fresh SSA. Tervahattu et al. (2002) found that organic films on SSA are common in fresh marine aerosols because of bursting bubbles from the spay of the waves. Quinn et al. (2015) also found that fresh SSA are internally mixed with organic matter in the northeastern Atlantic atmosphere using proton nuclear magnetic resonance (^{1}HNMR). In comparison with particle 1, the $^{12}C^{14}N^-$ intensity of the aged particles 2 and 3 was much enhanced. The only explanation is that more organic matter from the atmosphere was incorporated into the aged SSA. We also found organic contents are largely different from particle to particle based on the $^{12}C^{14}N^-$ intensity in particles 2 and 3 (Fig. 8b). Similar phenomena in aged SSA have been observed by laser mass spectrometry at Cape Grim and the amounts of additional sulfate and organic matter in individual particles may be an indication of particles ageing (Middlebrook et al., 1998). Additionally, with increasing organic matter in SSA, their morphology and crystallization behavior changes (Ault et al., 2013b).

Interestingly, $^{12}C^{14}N^-$ line scans in particles 2 and 3 further indicate that organic matter is mostly restricted to their surfaces (Fig. 8). The near edge X-ray absorption fine structure spectroscopy (NEXAFS) carbon K-edge spectrum of the organic phase reveals a dominant contribution from carboxylic acids on the surface of the aged SSA (Laskin et al., 2012). Ault et al. (2013a) showed that organic acids and nitrate are mainly concentrated on the surface after heterogeneous reactions between SSA and nitric acid in laboratory experiments. We further found Na_2SO_4 is present mainly in the core and organic matter internally mixed with nitrate on the surface for aged SSA in the natural arctic atmosphere. This finding supports the results from laboratory experiments and conforms to predictions of liquid–liquid phase separation theory (Ault et al., 2013a). As a result, we obtained one conceptual model based on these above findings summarizing the possible SSA ageing processes in the atmosphere (Fig. 9).

The nanoSIMS analyses of the aged SSA in the arctic air show that their surface layers commonly contain organic matter, although the organic content is largely different in different aged SSA. The organic layer may influence trace gas uptake, and subsequently impact trace gas budgets of O_3 and NO_2 in the arctic (McNeill et al., 2006). This is the first demonstration of organic-coated SSA in clean arctic air, which extends the application of heterogeneous reactions on aerosol particles (Fig. 9). Comparisons of fresh and aged SSA in Fig. 8 suggest that these organic coatings likely took part in the chloride depletion during particles ageing. The chloride depletion in the SSA induced by the presence of organic matter should be incorporated into the atmospheric chemistry models for clean marine air, in addition to the coastal urban regions reported by Laskin et al. (2012). Randles et al. (2014) reported that NaCl internally mixed with organic matter can reduce radiative cooling substantially compared to pure NaCl aerosol in the laboratory. In addition, how the organic layer influences hygroscopic and optical properties of the aged SSA in realistic atmospheres remains unknown. Our measurements make clear the need to understand SSA's complexity in arctic air.

5 Conclusions

TEM observations indicated that SSA were most abundant from 100 nm to 10 µm in the summer arctic atmosphere, accounting for about 72 % of the total aerosol particles. Three types of SSA, fresh SSA, partially aged SSA, and fully aged SSA, were identified based on their morphology and composition. The fresh SSA particles exhibited a single core-shell structure. Containing only Na and Cl, the core consisted of the cubic NaCl crystal with the coating of Mg, Ca, S, O and Cl, identified as $CaSO_4$ and $MgCl_2$. Individual partially aged SSA particles consisted of the single irregularly shaped NaCl core coated with Na, Mg, Ca, K, N, O, and S, with or without minor Cl, suggesting a single Cl-depletion phenomenon in the formation of partially aged SSA. The fully aged SSA lack the NaCl core, suggesting that the Cl in SSA was completely depleted through heterogeneous chemical reactions. Nonetheless, most fully aged SSA consist of the Na_2SO_4 core with the amorphous $NaNO_3$ coating.

STEM further determined the elemental mappings of Na, Mg, Ca, Cl, S, O, C, and N in the three kinds of SSA. We found that Cl content decreases and S, O, C and N contents increase along with particles ageing from partially to fully aged SSA. This result provides direct evidence that sulfate and nitrate formed in SSA through atmospheric chemical reactions in arctic area. In addition, $MgCl_2$ coating on fresh SSA can induce heterogeneous reactions between SSA and acidic gases because $MgCl_2$ is known to readily deliquesce at a point considerably lower (33 % RH at 298 K) than that of NaCl (75 %). The partially and fully aged SSA were expected to have liquid surfaces ($MgSO_4$, $MgNO_3$, and $NaNO_3$) in arctic ambient air (56–94 % RH); such surfaces contain substantial amounts of water, so the coating contents were conducive to accelerate the heterogeneous reactions. NanoSIMS technology has been employed to obtain secondary ion intensity mappings of $^{32}S^-$, $^{12}C^{14}N^-$, $^{23}Na^{16}O^-$, $^{35}Cl^-$, and $^{16}O^-$. $^{12}C^{14}N^-$ mapping and line scans of individual fresh SSA indicate extremely small amounts of organic matter in the coating of the particle, although this organic matter was somewhat enhanced in the aged SSA. We also found that organic matter was mostly limited to the particle surface. The chloride depletion in the SSA induced by the presence of organic matter should be incorporated into the atmospheric chemistry models for clean marine air. Our measurements exemplify the need to understand the complexity of realistic atmospheric SSA in the arctic.

The composition of the SSA and their internal heterogeneity likely have important effects on their hygroscopic and optical properties, dynamics of phase separations, and heterogeneous reaction with inorganic and organic acidic gases. These microscopic observations for SSA provide insights into the system of gas-aerosol-climate in the arctic atmosphere.

The Supplement related to this article is available online at doi:10.5194/acpd-15-16715-2015-supplement.

Acknowledgements. We appreciate Peter Hyde's comments and proofreading. This work was funded by Shandong Natural Science Funds for Distinguished Young Scholar (JQ201413), National Basic Research Program of China (2011CB403401), National Natural Science Foundation of China (41275141), China Polar Science Strategy Research Foundation (20140310), and Fundamental Research Funds of Shandong University (2014QY001). We gratefully acknowledge the NOAA Air Resources Laboratory (ARL) for the provision of the HYSPLIT transport used in this publication.

References

Allen, H. C., Laux, J. M., Vogt, R., Finlayson-Pitts, B. J., and Hemminger, J. C.: Water-induced reorganization of ultrathin nitrate films on NaCl:fiimplications for the tropospheric chemistry of sea salt particles, J. Phys. Chem., 100, 6371–6375, doi:10.1021/jp953675a, 1996.

Andreae, M. O., Charlson, R. J., Bruynseels, F., Storms, H., Van Grieken, R., and Maeahaut, W.: Internal mixture of sea salt, silicates, and excess sulfate in marine aerosols, Science, 232, 1620–1623, 1986.

Ault, A. P., Peters, T. M., Sawvel, E. J., Casuccio, G. S., Willis, R. D., Norris, G. A., and Grassian, V. H.: Single-particle SEM-EDX analysis of iron-containing coarse particulate matter in an urban environment: sources and distribution of iron within Cleveland, Ohio, Environ. Sci. Technol., 46, 4331–4339, 2012.

Ault, A. P., Guasco, T. L., Ryder, O. S., Baltrusaitis, J., Cuadra-Rodriguez, L. A., Collins, D. B., Ruppel, M. J., Bertram, T. H., Prather, K. A., and Grassian, V. H.: Inside versus outside: ion redistribution in nitric acid reacted sea spray aerosol particles as determined by single particle analysis, J. Am. Chem. Soc., 135, 14528–14531, doi:10.1021/ja407117x, 2013a.

Ault, A. P., Moffet, R. C., Baltrusaitis, J., Collins, D. B., Ruppel, M. J., Cuadra-Rodriguez, L. A., Zhao, D., Guasco, T. L., Ebben, C. J., Geiger, F. M., Bertram, T. H., Prather, K. A., and Grassian, V. H.: Size-dependent changes in sea spray aerosol composition and properties with different seawater conditions, Environ. Sci. Technol., 47, 5603–5612, doi:10.1021/es400416g, 2013b.

Barrie, L. A.: Arctic air pollution: an overview of current knowledge, Atmos. Environ., 20, 643–663, 1986.

Chang, R. Y.-W., Leck, C., Graus, M., Müller, M., Paatero, J., Burkhart, J. F., Stohl, A., Orr, L. H., Hayden, K., Li, S.-M., Hansel, A., Tjernström, M., Leaitch, W. R., and Abbatt, J. P. D.: Aerosol composition and sources in the central Arctic Ocean during ASCOS, Atmos. Chem. Phys., 11, 10619–10636, doi:10.5194/acp-11-10619-2011, 2011.

Conny, J. M. and Norris, G. A.: Scanning electron microanalysis and analytical challenges of mapping elements in urban atmospheric particles, Environ. Sci. Technol., 45, 7380–7386, 2011.

De Haan, D. O., Brauers, T., Oum, K., Stutz, J., Nordmeyer, T., and Finlayson-Pitts, B. J.: Heterogeneous chemistry in the troposphere: experimental approaches and applications to the chemistry of sea salt particles, Int. Rev. Phys. Chem., 18, 343–385, 1999.

Gard, E. E., Kleeman, M. J., Gross, D. S., Hughes, L. S., Allen, J. O., Morrical, B. D., Fergenson, D. P., Dienes, T., Gälli, M. E., and Johnson, R. J.: Direct observation of heterogeneous chemistry in the atmosphere, Science, 279, 1184–1187, 1998.

Geng, H., Ryu, J., Jung, H.-J., Chung, H., Ahn, K.-H., and Ro, C.-U.: Single-particle characterization of summertime arctic aerosols collected at Ny-Ålesund, Svalbard, Environ. Sci. Technol., 44, 2348–2353, doi:10.1021/es903268j, 2010.

Ghorai, S., Wang, B., Tivanski, A., and Laskin, A.: Hygroscopic properties of internally mixed particles composed of NaCl and water-soluble organic acids, Environ. Sci. Technol., 48, 2234–2241, doi:10.1021/es404727u, 2014.

Goto-Azuma, K. and Koerner, R. M.: Ice core studies of anthropogenic sulfate and nitrate trends in the Arctic, J. Geophys. Res.-Atmos., 106, 4959–4969, doi:10.1029/2000jd900635, 2001.

Hara, K., Yamagata, S., Yamanouchi, T., Sato, K., Herber, A., Iwasaka, Y., Nagatani, M., and Nakata, H.: Mixing states of individual aerosol particles in spring Arctic troposphere during ASTAR 2000 campaign, J. Geophys. Res.-Atmos., 108, 4209, doi:10.1029/2002jd002513, 2003.

Hara, K., Osada, K., Yabuki, M., and Yamanouchi, T.: Seasonal variation of fractionated sea-salt particles on the Antarctic coast, Geophys. Res. Lett., 39, L18801, doi:10.1029/2012gl052761, 2012.

Hegg, D. A., Warren, S. G., Grenfell, T. C., Doherty, S. J., Larson, T. V., and Clarke, A. D.: Source attribution of black carbon in Arctic snow, Environ. Sci. Technol., 43, 4016–4021, doi:10.1021/es803623f, 2009.

Heintzenberg, J.: Particle size distribution and optical properties of Arctic haze, Tellus, 32, 251–260, 1980.

Hu, D., Qiao, L., Chen, J., Ye, X., Yang, X., Cheng, T., and Fang, W.: Hygroscopicity of inorganic aerosols: size and relative humidity effects on the growth factor, Aerosol Air Qual. Res., 10, 255–264, 2010.

Hu, R. M., Blanchet, J. P., and Girard, E.: Evaluation of the direct and indirect radiative and climate effects of aerosols over the western Arctic, J. Geophys. Res.-Atmos., 110, D11213, doi:10.1029/2004jd005043, 2005.

Iziomon, M. G., Lohmann, U., and Quinn, P. K.: Summertime pollution events in the Arctic and potential implications, J. Geophys. Res.-Atmos., 111, D12206, doi:10.1029/2005jd006223, 2006.

Knipping, E. M., Lakin, M. J., Foster, K. L., Jungwirth, P., Tobias, D. J., Gerber, R. B., Dabdub, D., and Finlayson-Pitts, B. J.: Experiments and simulations of ion-enhanced interfacial chemistry on aqueous NaCl aerosols, Science, 288, 301–306, doi:10.1126/science.288.5464.301, 2000.

Kouyoumdjian, H. and Saliba, N. A.: Mass concentration and ion composition of coarse and fine particles in an urban area in Beirut: effect of calcium carbonate on the absorption of nitric and sulfuric acids and the depletion of chloride, Atmos. Chem. Phys., 6, 1865–1877, doi:10.5194/acp-6-1865-2006, 2006.

Laskin, A., Moffet, R. C., Gilles, M. K., Fast, J. D., Zaveri, R. A., Wang, B., Nigge, P., and Shutthanandan, J.: Tropospheric chemistry of internally mixed sea salt and organic particles: surprising reactivity of NaCl with weak organic acids, J. Geophys. Res.-Atmos., 117, D15302, doi:10.1029/2012jd017743, 2012.

Law, K. S. and Stohl, A.: Arctic Air Pollution: origins and impacts, Science, 315, 1537–1540, doi:10.1126/science.1137695, 2007.

Leck, C. and Svensson, E.: Importance of aerosol composition and mixing state for cloud droplet activation over the Arctic pack ice in summer, Atmos. Chem. Phys., 15, 2545–2568, doi:10.5194/acp-15-2545-2015, 2015.

Lee, C.-T., and Hsu, W.-C.: The measurement of liquid water mass associated with collected hygroscopic particles, J. Aerosol Sci., 31, 189–197, 2000.

Li, W., Li, P., Sun, G., Zhou, S., Yuan, Q., and Wang, W.: Cloud residues and interstitial aerosols from non-precipitating clouds over an industrial and urban area in northern China, Atmos. Environ., 45, 2488–2495, 2011a.

Li, W., Shao, L., Shen, R., Yang, S., Wang, Z., and Tang, U.: Internally mixed sea salt, soot, and sulfates at Macao, a coastal city in South China, JAPCA J. Air Waste Ma., 61, 1166–1173, doi:10.1080/10473289.2011.603996, in press, 2011b.

Li, W., Wang, T., Zhou, S., Lee, S., Huang, Y., Gao, Y., and Wang, W.: Microscopic observation of metal-containing particles from Chinese continental outflow observed from a non-Industrial site, Environ. Sci. Technol., 47, 9124–9131, doi:10.1021/es400109q, 2013a.

Li, W., Wang, Y., Collett, J. L., Chen, J., Zhang, X., Wang, Z., and Wang, W.: Microscopic evaluation of trace metals in cloud droplets in an acid precipitation region, Environ. Sci. Technol., 47, 4172–4180, doi:10.1021/es304779t, 2013b.

Li, W. J. and Shao, L. Y.: Transmission electron microscopy study of aerosol particles from the brown hazes in northern China, J. Geophys. Res.-Atmos., 114, D09302, doi:10.1029/2008JD011285, 2009.

Li, X. H., Zhao, L. J., Dong, J. L., Xiao, H. S., and Zhang, Y. H.: Confocal Raman studies of $Mg(NO_3)_2$ aerosol particles deposited on a quartz substrate: supersaturated structures and complicated phase transitions, J. Phys. Chem. B, 112, 5032–5038, doi:10.1021/jp709938x, 2008.

Lindsay, R., Zhang, J., Schweiger, A., Steele, M., and Stern, H.: Arctic sea ice retreat in 2007 follows thinning trend, J. Climate, 22, 165–176, 2009.

Liu, Y., Cain, J. P., Wang, H., and Laskin, A.: Kinetic study of heterogeneous reaction of deliquesced NaCl particles with gaseous HNO_3 using particle-on-substrate stagnation flow reactor approach, J. Phys. Chem. A, 111, 10026–10043, doi:10.1021/jp072005p, 2007.

McNeill, V. F., Patterson, J., Wolfe, G. M., and Thornton, J. A.: The effect of varying levels of surfactant on the reactive uptake of N_2O_5 to aqueous aerosol, Atmos. Chem. Phys., 6, 1635–1644, doi:10.5194/acp-6-1635-2006, 2006.

Middlebrook, A. M., Murphy, D. M., and Thomson, D. S.: Observations of organic material in individual marine particles at Cape Grim during the First Aerosol Characterization Experiment (ACE 1), J. Geophys. Res.-Atmos., 103, 16475–16483, doi:10.1029/97jd03719, 1998.

Murphy, D. M., Anderson, J. R., Quinn, P. K., McInnes, L. M., Brechtel, F. J., Kreidenweis, S. M., Middlebrook, A. M., Posfai, M., Thomson, D. S., and Buseck, P. R.: Influence of sea-salt on aerosol radiative properties in the southern ocean marine boundary layer, Nature, 392, 62–65, 1998.

O'Dowd, C. D. and De Leeuw, G.: Marine aerosol production: a review of the current knowledge, Philos. T. R. Soc. A, 365, 1753–1774, 2007.

O'Dowd, C. D., Smith, M. H., Consterdine, I. E., and Lowe, J. A.: Marine aerosol, sea-salt, and the marine sulphur cycle: a short review, Atmos. Environ., 31, 73–80, 1997.

Oum, K. W., Lakin, M. J., DeHaan, D. O., Brauers, T., and Finlayson-Pitts, B. J.: Formation of molecular chlorine from the photolysis of ozone and aqueous sea-salt particles, Science, 279, 74–76, doi:10.1126/science.279.5347.74, 1998.

Pósfai, M., Anderson, J. R., Buseck, P. R., Shattuck, T. W., and Tindale, N. W.: Constituents of a remote pacific marine aerosol: a TEM study, Atmos. Environ., 28, 1747–1756, 1994.

Park, K., Kim, G., Kim, J.-s., Yoon, Y.-J., Cho, H.-j., and Ström, J.: Mixing state of size-selected submicrometer particles in the Arctic in May and September 2012, Environ. Sci. Technol., 48, 909–919, doi:10.1021/es404622n, 2014.

Quinn, P. K., Collins, D. B., Grassian, V. H., Prather, K. A., and Bates, T. S.: Chemistry and related properties of freshly emitted sea spray aerosol, Chem. Rev., doi:10.1021/cr500713g, 2015.

Rastak, N., Silvergren, S., Zieger, P., Wideqvist, U., Ström, J., Svenningsson, B., Maturilli, M., Tesche, M., Ekman, A. M. L., Tunved, P., and Riipinen, I.: Seasonal variation of aerosol water uptake and its impact on the direct radiative effect at Ny-Ålesund, Svalbard, Atmos. Chem. Phys., 14, 7445–7460, doi:10.5194/acp-14-7445-2014, 2014.

Rossi, M. J.: Heterogeneous reactions on salts, Chem. Rev., 103, 4823–4882, 2003.

Sand, M., Berntsen, T. K., Kay, J. E., Lamarque, J. F., Seland, Ø., and Kirkevåg, A.: The Arctic response to remote and local forcing of black carbon, Atmos. Chem. Phys., 13, 211–224, doi:10.5194/acp-13-211-2013, 2013.

Serreze, M. C. and Francis, J. A.: The Arctic amplification debate, Climatic Change, 76, 241–264, 2006.

Shaw, G. E.: The Arctic haze phenomenon, B. Am. Meteorol. Soc., 76, 2403–2413, 1995.

Sierau, B., Chang, R. Y.-W., Leck, C., Paatero, J., and Lohmann, U.: Single-particle characterization of the high-Arctic summertime aerosol, Atmos. Chem. Phys., 14, 7409–7430, doi:10.5194/acp-14-7409-2014, 2014.

Tervahattu, H., Hartonen, K., Kerminen, V. M., Kupiainen, K., Aarnio, P., Koskentalo, T., Tuck, A. F., and Vaida, V.: New evidence of an organic layer on marine aerosols, J. Geophys. Res.-Atmos., 107, 4053, doi:10.1029/2000jd000282, 2002.

Vavrus, S.: The impact of cloud feedbacks on Arctic climate under greenhouse forcing, J. Climate, 17, 603–615, 2004.

Wise, M. E., Freney, E. J., Tyree, C. A., Allen, J. O., Martin, S. T., Russell, L. M., and Buseck, P. R.: Hygroscopic behavior and liquid-layer composition of aerosol particles generated from natural and artificial seawater, J. Geophys. Res.-Atmos., 114, D03201, doi:10.1029/2008jd010449, 2009.

Woods, E., Chung, D., Lanney, H. M., and Ashwell, B. A.: Surface morphology and phase transitions in mixed NaCl/$MgSO_4$ aerosol particles, J. Phys. Chem. A, 114, 2837–2844, doi:10.1021/jp911133j, 2010.

Yao, X. and Zhang, L.: Chemical processes in sea-salt chloride depletion observed at a Canadian rural coastal site, Atmos. Environ., 46, 189–194, doi:10.1016/j.atmosenv.2011.09.081, 2011.

Zhao, L. J., Zhang, Y. H., Wei, Z. F., Cheng, H., and Li, X. H.: Magnesium sulfate aerosols studied by FTIR spectroscopy: hygroscopic properties, supersaturated structures, and implications for seawater aerosols, J. Phys. Chem. A, 110, 951–958, 2006.

ACPD
15, 16715–16745, 2015

Heterogeneous reactions of Arctic Sea salts

J. W. Chi et al.

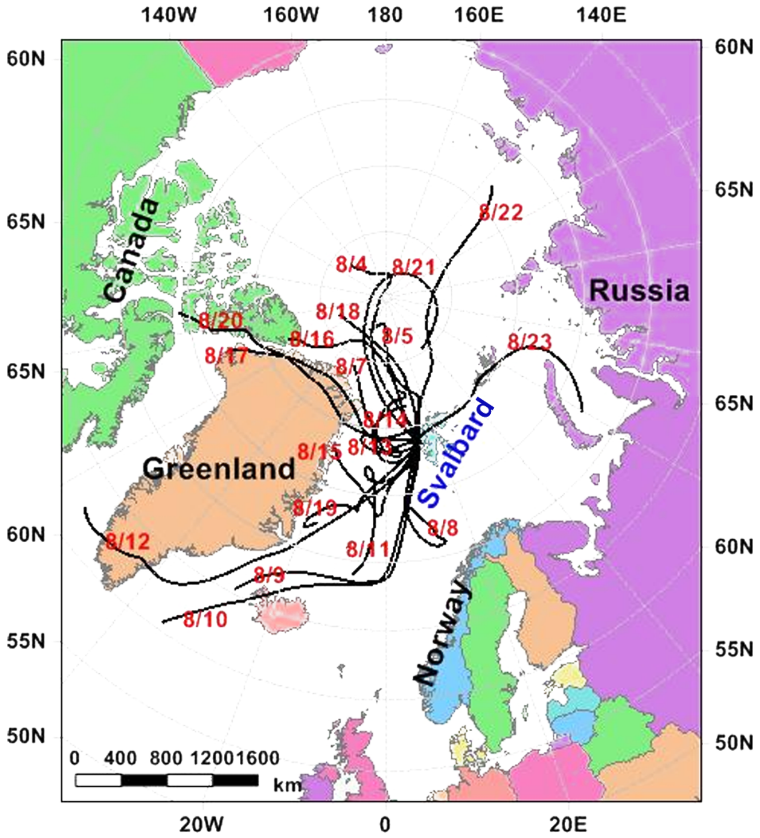

Figure 1. 72 h backward air mass trajectories at 500 m over Arctic Yellow River Station in Svalbard during 3 August to 23 August 2012.

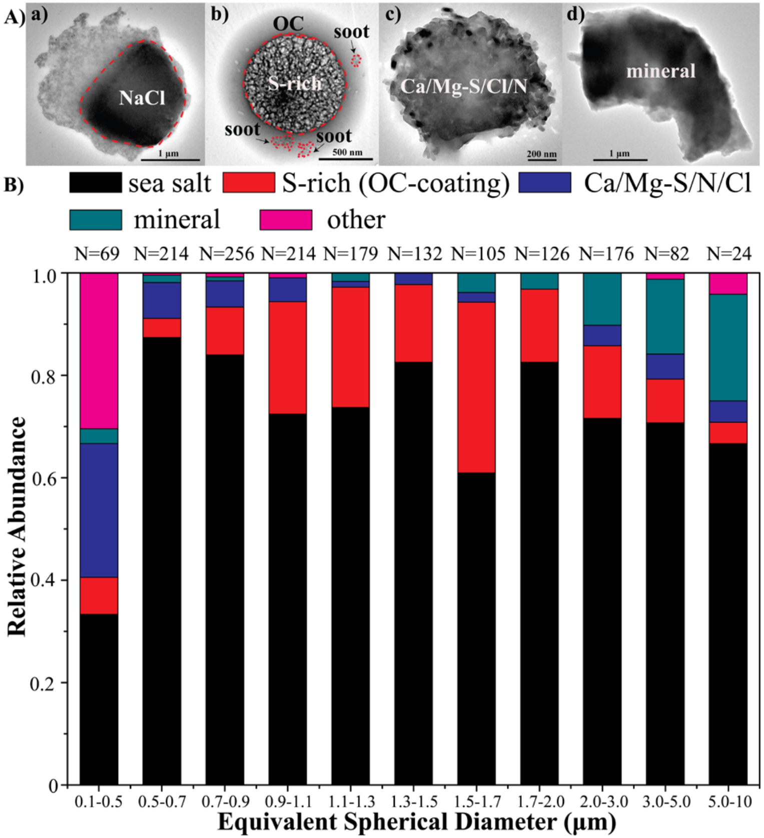

Figure 2. Morphology and relative abundances of typical individual aerosol particles in summertime Arctic samples: **(a)** TEM images of four types of aerosol particles, **(b)** relative abundances of different particle size ranges.

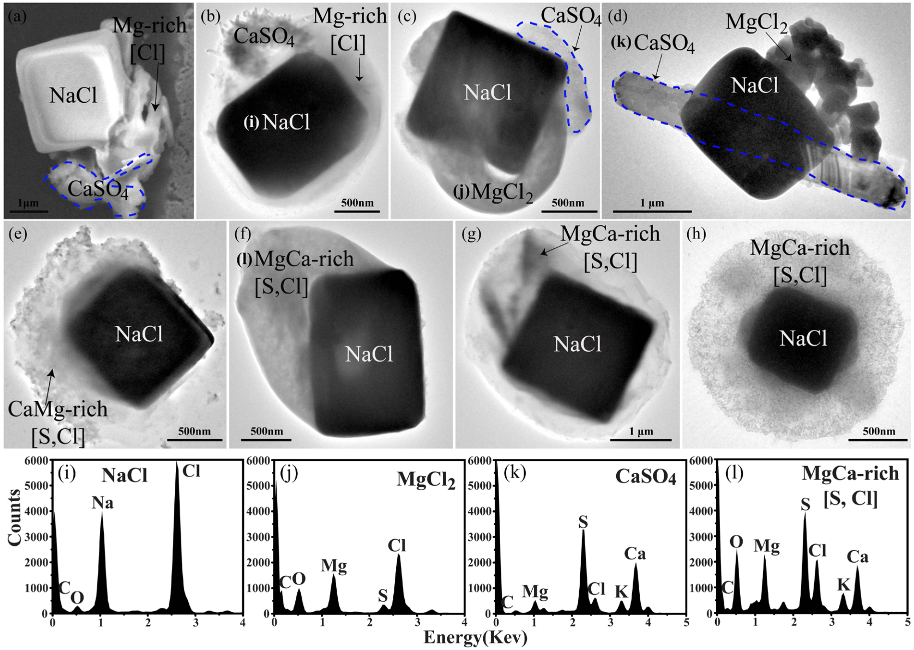

Figure 3. Morphology and EDX spectra of the typical fresh SSA. **(a)** One SEM image, **(b–h)** TEM images, and **(i–h)** EDX spectra of NaCl, $MgCl_2$, $CaSO_4$, and MgCa-rich. The main anionic elements are shown in the square brackets.

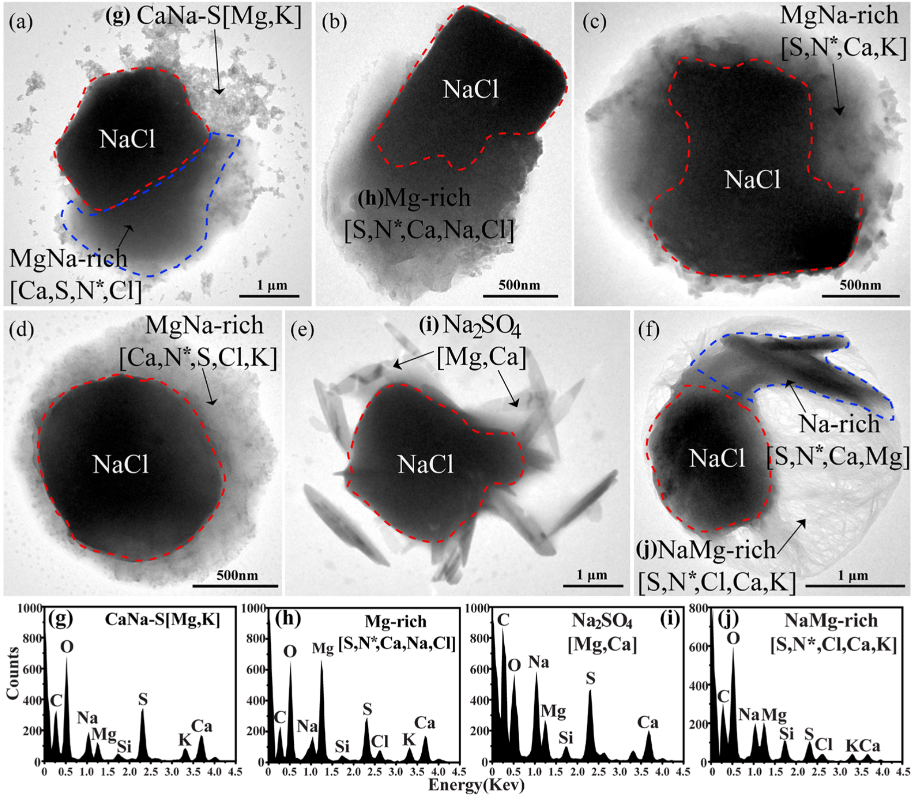

Figure 4. TEM images of typical partially aged SSA and EDX spectra of their coatings. **(a–b)** NaCl partially surrounded by the mixed species, containing Mg, Ca, Na, S, O, N and minor Cl; **(c–d)** NaCl completely surrounded by the mixed species with Mg, Ca, Na, S, O, N and minor Cl; **(e–f)** The rod-like Na_2SO_4 particles (minor Mg, and Ca) associated with NaCl. **(g–j)** The EDX spectra of one selected area in the internally mixed coating, including Na, Ca, Mg, S, and O with minor Cl and K. N content cannot be directly measured but has been inferred based on the probable aerosol components.

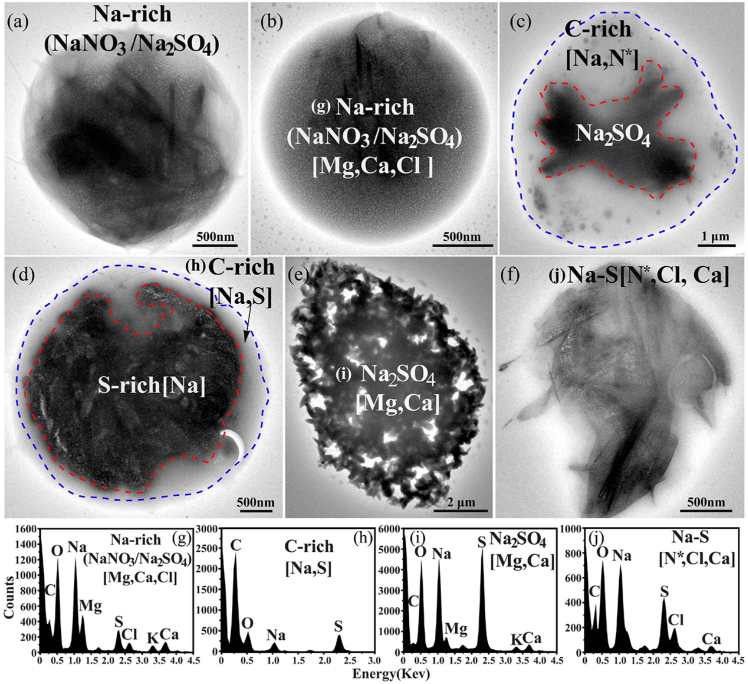

Figure 5. TEM images and EDX spectra of the typical fully aged SSA. Major species are shown in parentheses, and minor elements are in square brackets. **(a–b)** This Na-rich particle contains mostly Na, O, N, and S. The rod-like aggregates are Na_2SO_4 and the species of no-defined shape are $NaNO_3$. The $NaNO_3$-containing coating is more sensitive to the strong electron beam than the Na_2SO_4. **(c–d)** Na-rich particles mainly contain C, N, O, Na, and S. One typical transparent coating with high C and minor O, Na, S or N, was stable under a strong electron beam, suggesting a possible organic coating. **(e–f)** The particles mainly contain Na, O, and S. Many small rod-like Na_2SO_4 gather together to form one particle. **(g–j)** EDX spectra of one selected part within individual SSA marked in TEM images. N content cannot be directly measured but has been inferred based on its probable aerosol components.

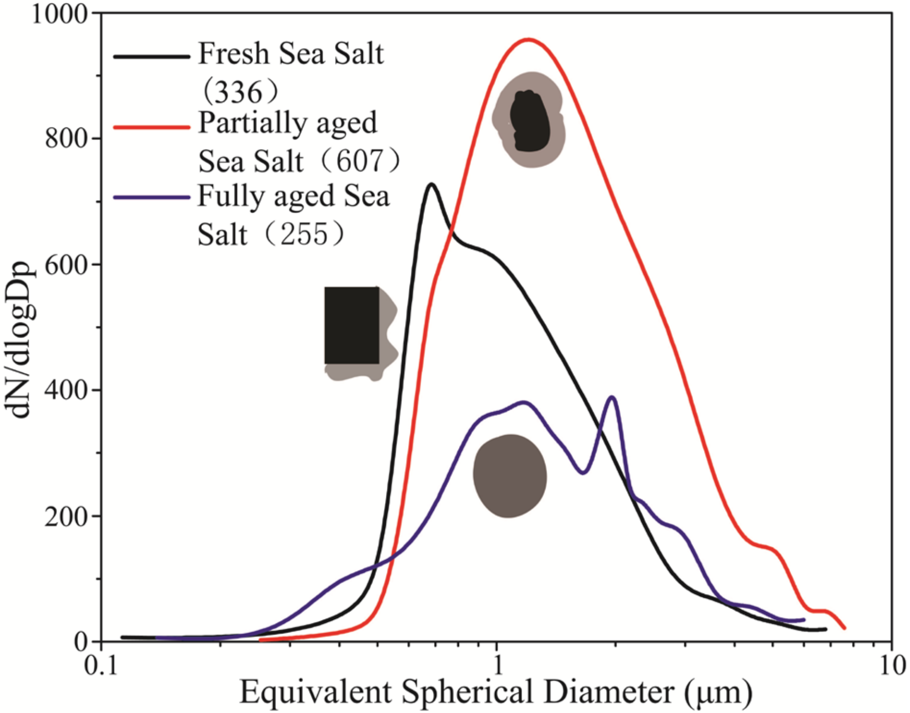

Figure 6. Size distributions of 336 fresh, 607 partially aged, and 255 fully aged SSA collected in Arctic summer. The SSA with diameter lower than 100 nm were not considered in this study.

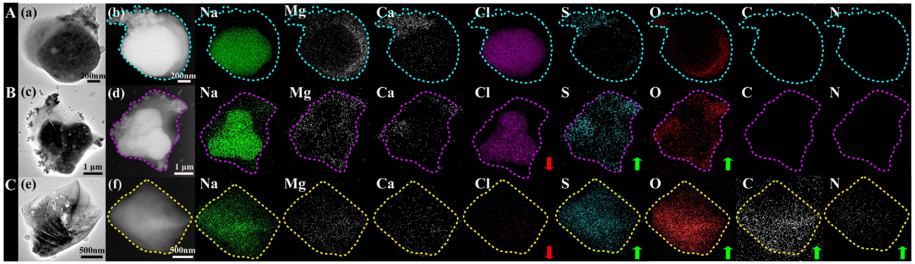

Figure 7. Bright and dark-field TEM images of the fresh, partially aged, and fully aged SSA and elemental mapping of Na, Mg, Ca, Cl, S, O, C, and N. **(a)** One fresh SSA particle, **(b)** one partially aged SSA particle, **(c)** one fully aged SSA particle. The dot intensity represents element concentration within an individual particle. The arrows in particles B and C represent the elemental concentration increase or decrease compared to the particle A.

Title Page
Abstract Introduction
Conclusions References
Tables Figures
◀◀ ▶▶
◀ ▶
Back Close
Full Screen / Esc
Printer-friendly Version
Interactive Discussion

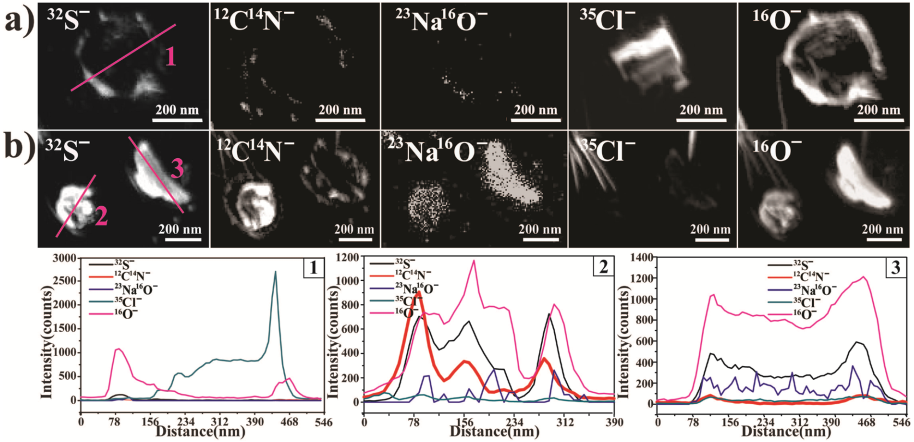

Figure 8. NanoSIMS-based ion intensity mappings. Mappings of $^{32}S^-$, $^{12}C^{14}N^-$, $^{23}Na^{16}O^-$, $^{35}Cl^-$, and $^{16}O^-$ from one fresh SSA particle **(a)** and two fully aged SSA **(b)**. Lines 1–3 represent the line scanning on the surfaces of individual particles. The red lines represent the profile of $^{12}C^{14}N^-$ in individual SSA.

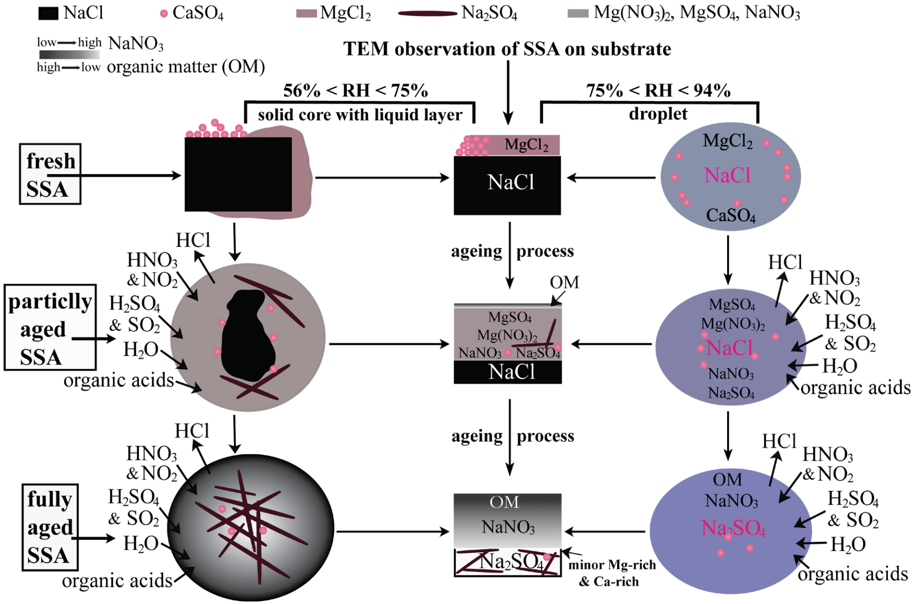

Figure 9. The conceptual model based on our study summarizing the possible SSA ageing processes from fresh, partially aged, and fully aged SSA. Deliquescence relative humidity (DRH) of NaCl is at 75 %. Ageing of SSA dominated by NaCl could have different processes before and after the DRH.